TRANSACTIONS OF THE INSTITUTE OF AVIATION **ISSN 0509-6669**
No. 1 (246), pp. 79-94, Warsaw 2017 **eISSN 2300-5408**

ANALYSIS OF HEAT TRANSFER IN A SUPERSONIC ROCKET HEAD

ADAM ROSŁOWICZ, PAWEŁ BEDNARCZYK

Rocketry Group of the Students' Space Association, Faculty of Power and Aeronautical Engineering, Warsaw University of Technology, Plac Politechniki 1, 00-661 Warsaw
adros@o2.pl, pawelbednarczyk91@o2.pl

Abstract

Design of supersonic H1 rocket by the Rocketry Group of Students' Space Association (SR SKA) requires an analysis of thermal phenomena occurring in the elements particularly exposed to the high temperature gas. This paper contains a description of the methodology and the results of numerical simulation of heat transfer in the elements of the rocket head. The starting points were the flight conditions (3 characteristic points defined by altitude and Mach number) and independently calculated adiabatic temperature field of the gas. ANSYS Fluent code was used to determine the temperature field on the surface of the rocket. Computed cases were viscous and inviscid flow (for comparison). Based on the results formulated for the viscous case heat transfer boundary conditions, the numerical model and the thermophysical properties of materials were defined. The model was limited to a brass top part of the head and a part of a composite dome. Analytical and empirical method of "intermediate enthalpy" determined distribution of the heat transfer coefficient on the rocket surface. Then the transient heat transfer was calculated with the ANSYS system. It included the range from the rocket launch, moment of maximum Mach number to sufficient structure cooling. The results of the analyses were conclusions relevant to the further development work. Excessive heating of composite structures during the flight has been shown.
Keywords: rocket technology, computational fluid mechanics, unsteady heat transfer, ANSYS software.

1. INTRODUCTION

The construction of the H1 ultrasonic rocket by SR SKA (Rocketry Section of the Students' Scientific Society) is associated with the need to analyse thermal phenomena occurring in the elements particularly exposed to contact with high temperature gas. The purpose of the analysis is to determine the temperature field and the heat flux in the head structure of the H1b sounding rocket. The computations performed with the use of the ANSYS system include the time period of the rocket's flight, during which significant thermal loads occur. Due to the assumed high flight velocity (up to Ma=3 maximum), the phenomena of heat transfer between air and the rocket structure play a big role and cannot be omitted. While defining the loads, the performance of the H1b rocket was analysed, as well as the flow around the head with the use of the FLUENT code. The flow analysis was conducted for a viscous model. In order to compare the results, the inviscid case was also computed. Temperature, pressure and Mach number were adapted for two assumed points of the flight trajectory. The geometry was simplified in the numerical model of the flow.

2. ROCKET HEAD SURFACE TEMPERATURE FIELD COMPUTATIONS

2.1. Geometry model and discretisation

A tetragonal, 2-dimensional, axisymmetric grid was created for the computations. The grid size is approx. 1.2 mln elements. In addition, the grid was condensed in the region of the shock wave formation. The rocket is inside a cuboidal computational space. Its size was selected so as to simulate the phenomena occurring in the flow well. The computational space extends by 3 lengths of the rocket to the front and 5 lengths of the rocket to the back. Figure 1 presents the visualisation of the computational grid.

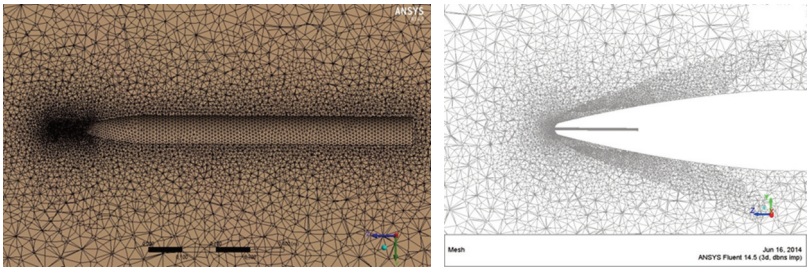

Fig. 1. Tetragonal grid of the model [Bednarczyk, 2014]

2.2. Solver settings in the Fluent system

The following settings were selected for inviscid flow:
- steady flow, compressible;
- inviscid fluid, energy equation included;
- boundary condition *pressure_far_field*, *Ma*=3.

Whereas, for viscous flow:
- steady flow, compressible;
- Spalart_Allmaras viscosity model, energy equation included;
- boundary condition *pressure_far_field*, *Ma*=3.

2.3. Comparison of the viscous and inviscid models

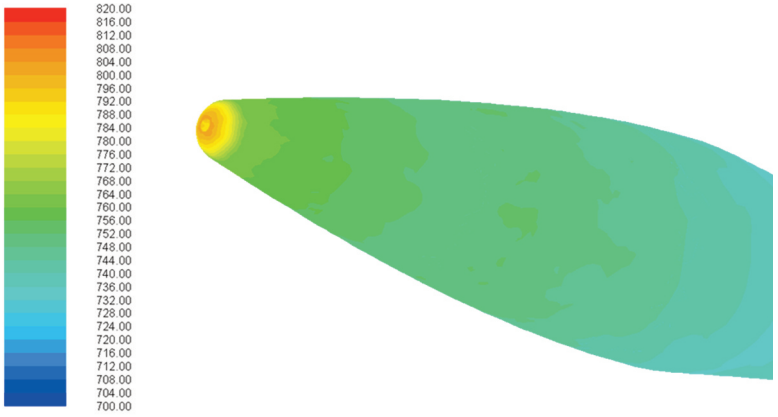

Fig. 2. Temperature distribution on the rocket head for the viscous case, in Kelvin. The scale covers a range from 700K to 820K [Bernaczyk, 2014].

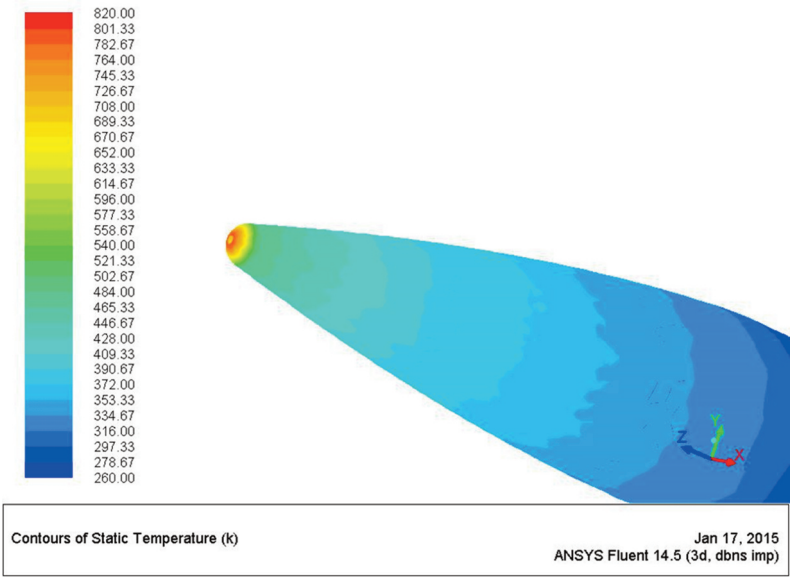

Fig. 3. Temperature distribution on the rocket head for the inviscid case, in Kelvin. The scale covers a range from 260K to 820K [Bernaczyk, 2014].

Different temperature scales were used during the presentation of the results. The reason for that is a large difference between the minimum temperature of the presented models. The temperature distribution in the inviscid model depends only on the flow stagnation, whereas, in the viscous model, it also depends on the friction of the fluid flowing around the rocket. In order to simulate the real phenomena as well as possible, the model with viscous flow was used in further computations.

2.4. Simulation results for M*a*=3.

The numerical simulation results for Ma=3 and the viscous model are presented below. It is the maximum anticipated Mach number during the flight of the rocket.

Fig. 4. Flow velocity map depicted in terms of the Mach number [Bednarczyk, 2014]

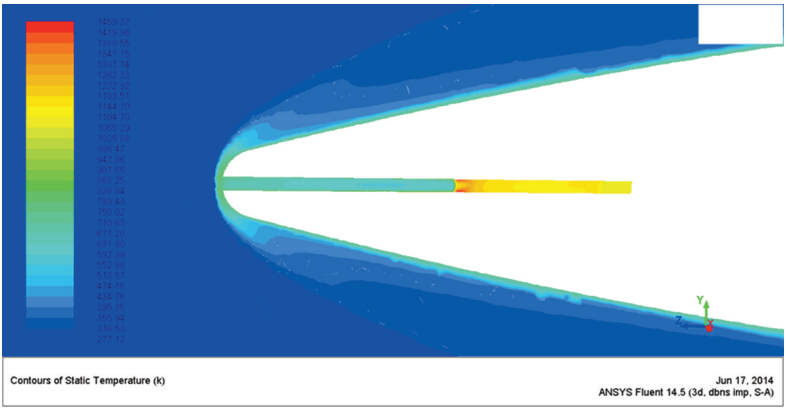

Fig.5. Map of temperature in the Prandtl tube (K) [Bednarczyk, 2014]

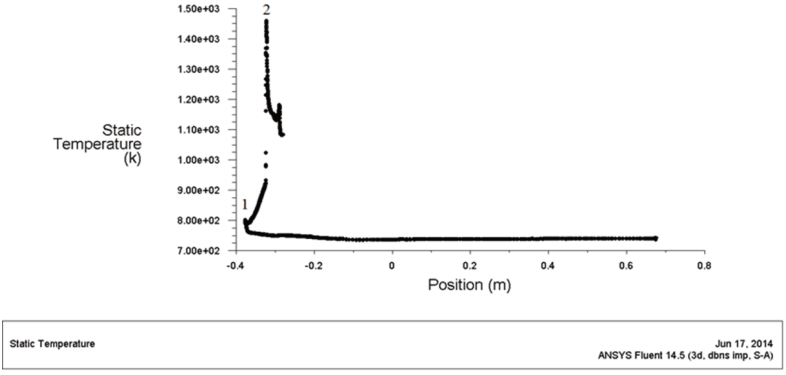

Fig. 6. Distribution of temperature vs rocket length. The head's coordinates are from -0.4m to -0.1m. Point 1 – stagnation point on the rocket head, point 2 – stagnation point in the Prandtl tube [Bednarczyk, 2014]

2.5. Simulation results for Ma=1.58.

The numerical simulation results for Ma=1.58 and the viscous model are presented below. At this value of the Mach number during the rocket decelerating, the stagnation temperature reaches the maximum allowable operational temperature limit of the composite.

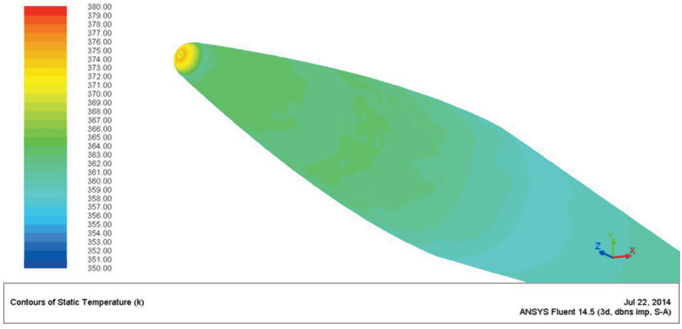

Fig. 7. Temperature distribution on the rocket head, in Kelvin [Bednarczyk, 2014]

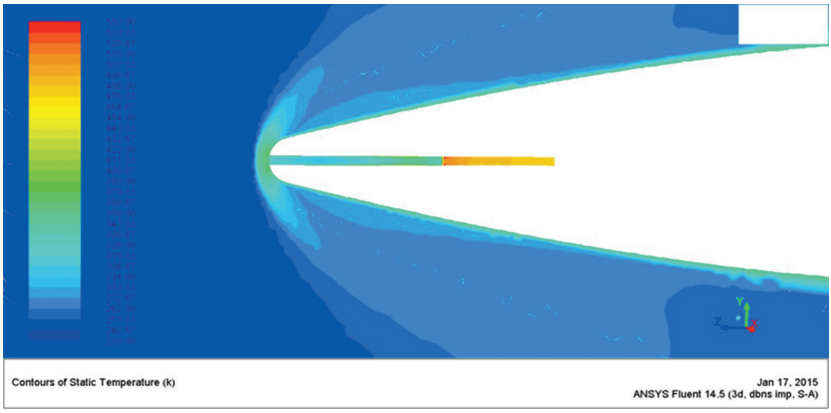

Fig. 8. Map of temperature in the Prandtl tube (K) [Bednarczyk, 2014]

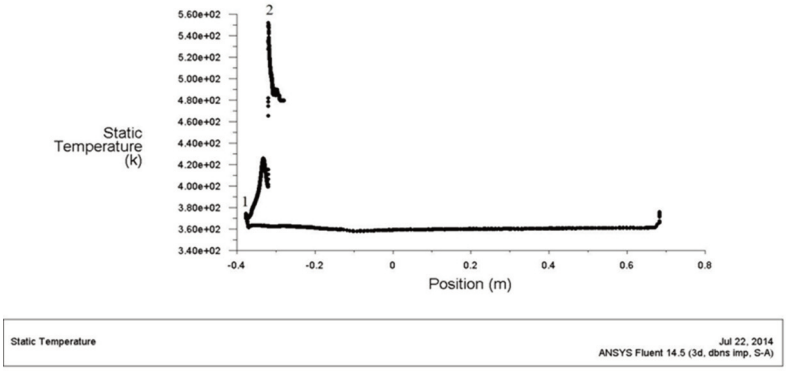

Fig. 9. Distribution of temperature vs rocket length. The head's coordinates are from -0.4m to -0.1m. Point 1 – stagnation point on the rocket head, point 2 – stagnation point in the Prandtl tube [Bednarczyk, 2014]

3. NUMERICAL HEAT TRANSFER ANALYSIS

3.1. Geometric model of the rocket head

The paper focuses on the analysis of heat transfer in head elements directly exposed to the impact of hot air, which are the brass tip and the composite dome.

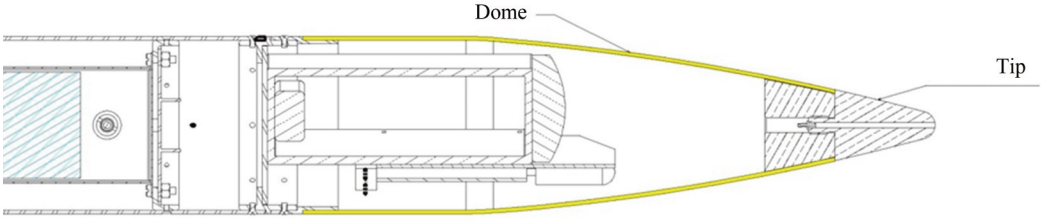

Fig. 10. Rocket head cross-section with marked analysed elements [SR SKA, 2014].

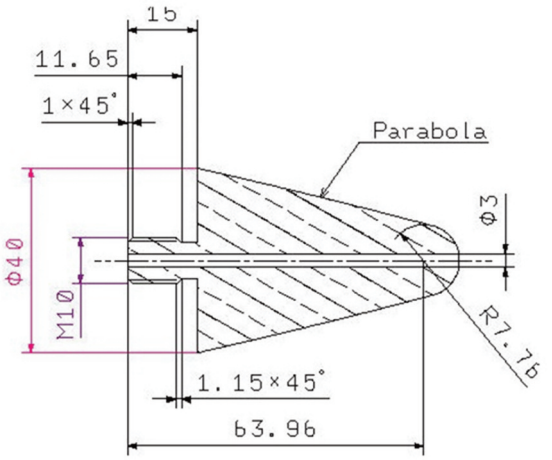

Fig. 11. Rocket tip [SR SKA, 2014]

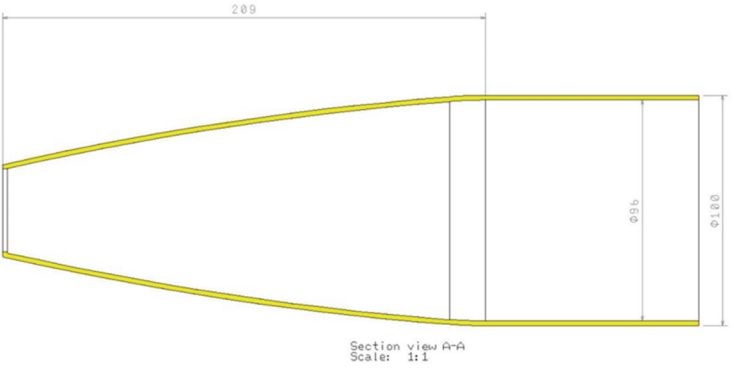

Fig. 12. Rocket dome [SR SKA, 2014]

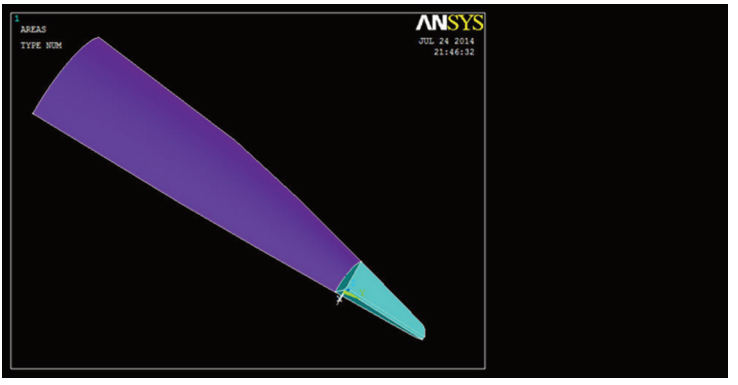

Fig. 13. The geometric model (3D axisymmetric) [Rosłowicz, 2014].

For the purposes of the heat transfer analysis model, it was decided to omit the threaded part of the tip, since it is located far from the most exposed areas. A conical shape of the tip with a semicircular end was assumed. The dome over the paraboloidal part was taken into account

(Fig. 12). Due to the axial symmetry of the case, heat transfer in the head quadrant was simulated. Creation a 2-dimensional model was impossible due to the character of the finite elements used for modelling the composite dome.

3.2. Rocket head computational grid

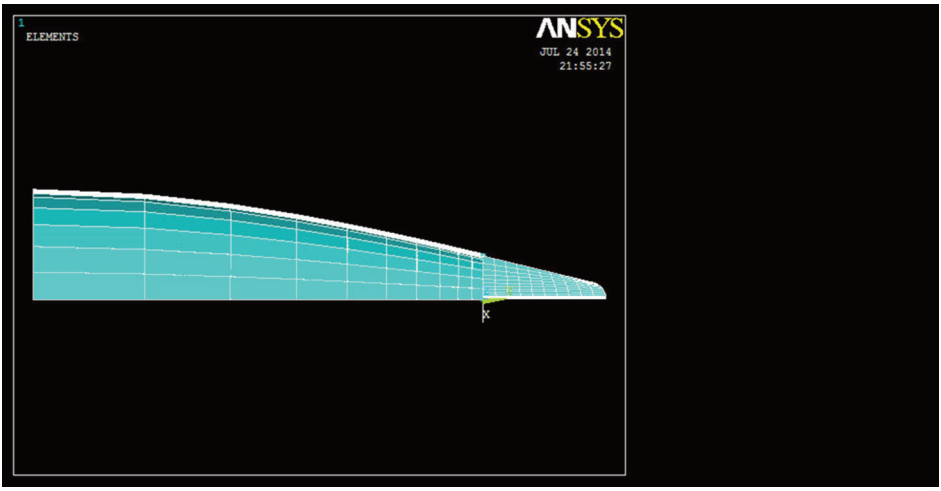

Fig. 14. A grid of finite elements [Rosłowicz, 2014]

3.3. Material properties of the rocket head

The thermo-physical material properties necessary to analyse heat transfer were defined. It was assumed they were constant.

Tab. 1. Thermo-physical properties of the head materials [SR SKA, 2014]

	Tip	**Dome**
Material	MO59	EPOLAM2080/glass fibre
Density, kg/m^3	8 430	2 800*
Specific heat, J/(kgK)	377	879
Thermal conductivity coefficient, W/(mK)	109.00	2.89**
Maximum operating temperature, °C	1 000	185

* on the basis of the rocket's technical documentation [1], ** based on [4], p. 1711, tab. 2., [GE material]

3.4. Heat transfer boundary conditions

During the flight, the rocket head is exposed to particularly high thermal loads. They result from the stagnation of flow during high-velocity flights. The flight profile and the adiabatic stagnation temperature curve were determined on the base of numerical calculations. Detailed information regarding the used model and numerical code can be found in the source material [7].

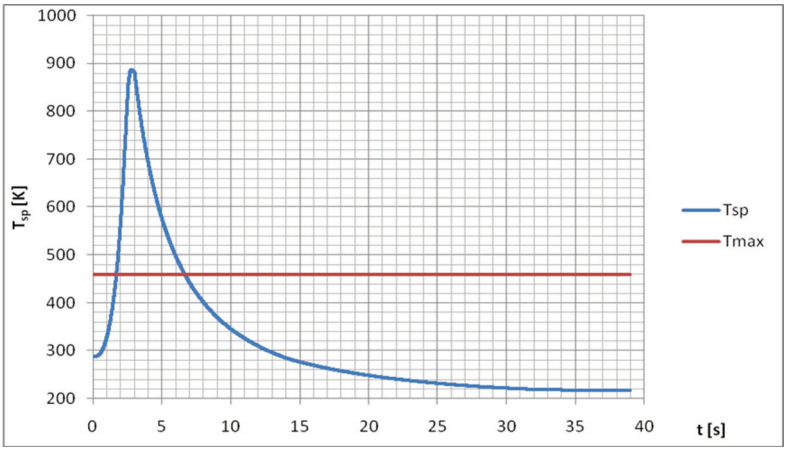

Fig. 15. The adiabatic stagnation temperature curve (axis *y*). Epoxy resin melting point was indicated. The flight time of the rocket is applied on axis *x* [Rosłowicz, 2014]

It was decided to determine the following heat transfer boundary conditions:

- Outer surface and Pitot tube – third-type condition (Fourier), forced convection, distribution of the fluid temperature and the heat transfer coefficient.
- Inner surfaces – second-type condition (Neumann), heat flux density distribution.
- Model symmetry surfaces and the bottom edge – adiabatic.

It was assumed that the analysed case was axisymmetric. Therefore, the boundary conditions are the function of coordinate *y* along the rocket axis and time. Coordinate *y*=0 means the tip bottom surface.

The temperature distribution on the outer surfaces and in the tube was obtained from the analysis of the flow around the head and for two points of the flight trajectory: 1 (*Ma*=3, *H*=1km) and 2 (*Ma*=1.58, *H*=6km).The figures show fluid temperature distribution and the evaluated approximating functions.

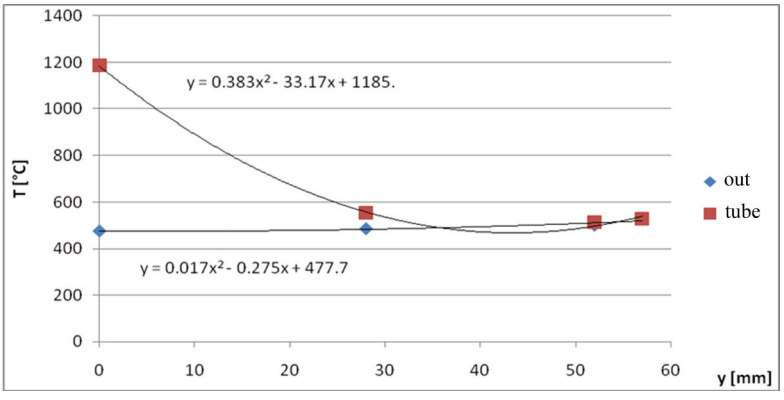

Fig. 16. Distribution of the adiabatic temperature of the fluid on the tube surface at *Ma*=3 (axis y), y is a coordinate calculated along the rocket axis from the base of the tip towards the end [Rosłowicz, 2014]

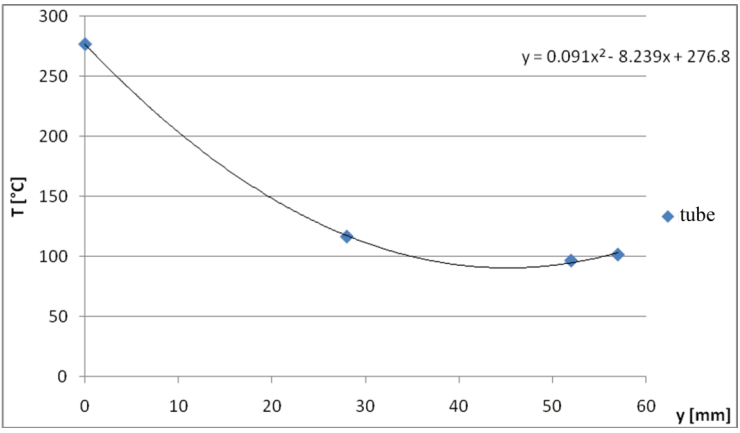

Fig. 17. Distribution of the adiabatic temperature of the fluid on the tube surface at $Ma = 1{,}58$ (axis y), y is a coordinate calculated along the rocket axis from the base of the tip to the end [Rosłowicz, 2014]

Flow analysis indicates that the fluid temperature at the dome surface changes slightly, therefore, a constant value was assumed in both cases. Similarly in case 2, constant (due to y) temperature values along the entire inner surface were assumed.

The heat transfer coefficient distribution was calculated with the use of the intermediate enthalpy method. The known distribution of fluid temperature without heat transfer with the structure, the Mach number fields and flight conditions (static pressure, kinematic viscosity) were used. Due to non-determined temperature of the structure during the flight, the computations were conducted iteratively.

For the purpose of calculating the current Reynolds number, an auxiliary coordinate s was introduced along the surface of the head, assuming that in approximation, it has the shape of a cone.

$$s = \frac{y'}{\cos\alpha} \tag{1}$$

where:
y' – axial coordinate calculated from the tip of the rocket, α – half-angle of line inclination of the head cone, $\alpha \approx 14°$.

The current Reynolds number was defined on this basis:

$$\mathrm{Re}_s = \frac{s u_\infty}{\nu_\infty} \tag{2}$$

where:
u_∞ – undisturbed velocity
ν_∞ – undisturbed kinetic viscosity

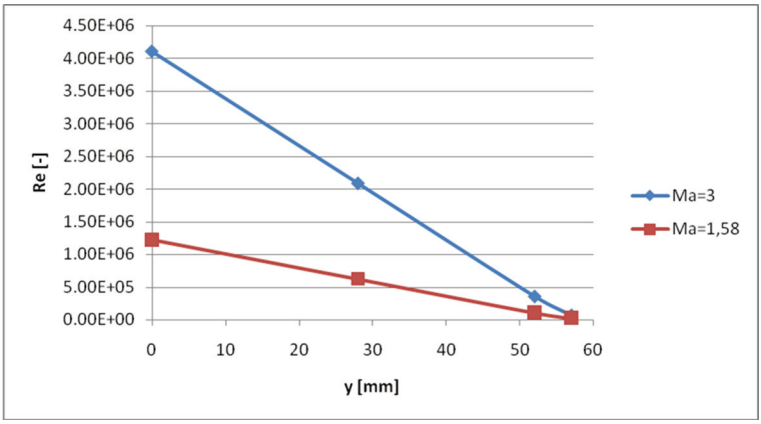

Fig. 18. Distribution of the current Reynolds number (axis *y*) along the rocket axis (axis *x*) [Rosłowicz, 2014]

Re=50000 is considered to be the boundary value of the outer laminar flow. On the basis of distribution analysis (fig. 18), it can be assumed that turbulent flow is present around the entire length of the head.

The following air properties were determined for the purposes of further calculations. Average values are related to the average temperature in the boundary layer.

Tab. 2. Properties of air in the outer flow around the head [Rosłowicz, 2014]

		1	**2**
Undisturbed velocity, m/s	u_∞	1 105	499
Kinematic viscosity of undisturbed flow, m^2/s	ν_∞	1.58×10^{-5}	2.40×10^{-5}
Boundary layer average temperature, °C	$T_{śr}$	500	90
Kinematic viscosity, m^2/s	$\nu_{śr}$	7.94×10^{-5}	2.21×10^{-5}
Thermal conductivity coefficient, W/(mK)	$\lambda_{śr}$	0.0574	0.0313
Specific heat, J/(kgK)	c_p	1 093	1 009
Adiabatic exponent	k	1.4	
Heat recovery coefficient	r	0.89	
Static pressure, Pa	p	85 600	47 200
Gas constant, J/(kgK)	R	287	

Based on the T_r fluid adiabatic temperature on the wall, enthalpy was determined:

$$i_r=T_r c_p \tag{3}$$

Enthalpy of the fluid on the edge of the boundary layer can be determined from the relationship:

$$\frac{i_r}{i_e}=1+r\frac{k-1}{2}Ma_e^2 \Rightarrow i_e=i_r\left(1+r\frac{k-1}{2}Ma_e^2\right)^{-1} \tag{4}$$

where:
Ma_e – local Mach number on the edge of the boundary layer.

Enthalpy on the wall was calculated similarly, by assuming further approximations of the boundary temperature T_w. The initial value was arbitrarily determined on the basis of launch conditions.

$$i_w = T_w c_p \tag{5}$$

Next, average enthalpy was calculated with the use of the empirical formula:

$$i^* = i_e + 0,5 \times \left(i_w - i_e\right) + 0,22 \times \left(i_r - i_e\right) \tag{6}$$

The corresponding temperature is:

$$T^* = \frac{i^*}{c_p} \tag{7}$$

Analogously:

$$T_e = \frac{i_e}{c_p} \tag{8}$$

The heat transfer coefficient was determined with the use of the Stanton number. The average value over the section from 0 to cross-section x is (for the minor difference between T_e and T^*):

$$\overline{St} = 0,28 \frac{T_e}{T^*} \log_{10}^{-2,6} \mathrm{Re}_s \tag{9}$$

The obtained value requires to be multiplied by 1.28 for the flow around cone.

Finally, the heat transfer coefficient was determined from the definition of the Stanton number:

$$St = \frac{\alpha_p}{\rho_e u_e c_p} \Rightarrow \alpha_p = \overline{St} \rho_e u_e c_p = \overline{St} \frac{p}{RT_e} \sqrt{kRT_e} Ma_e c_p \tag{10}$$

In the case of flow through a Pitot tube, a method based on the Nusselt number was used. The following empirical correlation was used:

$$Nu_D = 0,023 Re_D^{0,8} \mathrm{Pr}^n \tag{11}$$

where:
Re_D – Reynolds number based on the D tube diameter,
n=0.3 for wall heating; n=0.4 for wall cooling.

Tab. 3. Data for Pitot tube calculations [Rosłowicz, 2014]

		1	2
Tube diameter, (m)	D	0.003	
Average specific heat in the boundary layer, J/(kgK)	c_p	1 172	1 022
Average Prandtl number, -	Pr	0.690	0.681

The Re_D number was defined as:

$$\mathrm{Re}_D = \frac{Du_e}{\nu_e} \tag{12}$$

where:

u_e – flow velocity on the edge of the boundary layer,
v_e – kinemtatic viscosity on the edge of the boundary layer.

The heat transfer coefficient in the tube α_p was calculated from the definition of the Nusselt number Nu_D:

$$Nu_D = \frac{D\alpha_p}{\lambda_p} \Rightarrow \alpha_p = \frac{Nu_D \lambda_p}{D} \tag{13}$$

In the above-mentioned formula, the air heat transfer coefficient λ_p was read for the current temperature at the edge of the boundary layer.

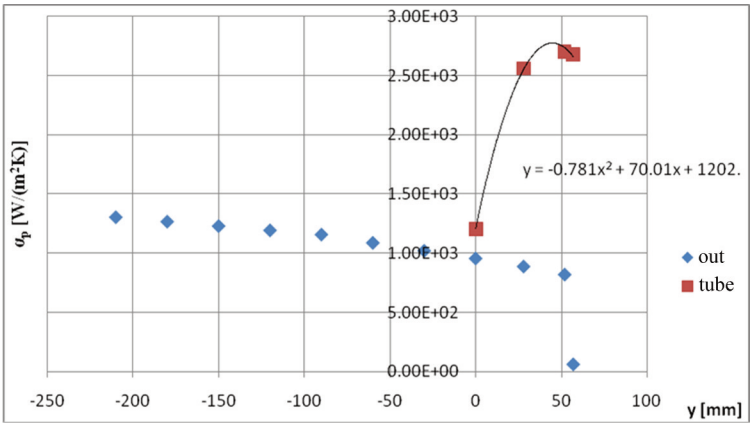

Fig. 19. The distribution of the heat transfer coefficient (axis *y*) along the coordinate *y* (axis *x*) for *Ma* = 3 and the approximating function [Rosłowicz, 2014]

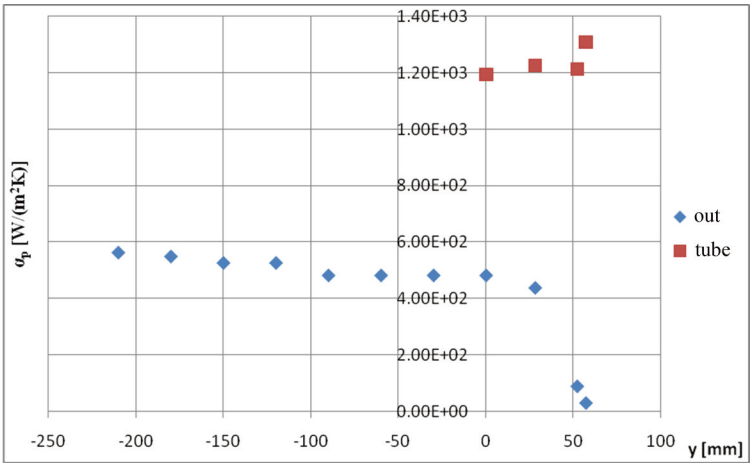

Fig. 20. The distribution of the heat transfer coefficient (axis *y*) along the coordinate *y* (axis *x*) for *Ma* = 1.58 [Rosłowicz, 2014]

The computed values of the heat transfer coefficient were verified on the basis of the results of theoretical and experimental studies in [2]. Average values from the entire length of the head were

adopted for the calculations, except for the stagnation tube at Ma = 3, for which the distribution was assumed with the use of an approximating function (fig. 19).

The heat flux densities on the outer surfaces of the structure were estimated on the basis of the amount of heat transferred from the fluid to the surface, according to Newton's law:

$$q = \alpha_p(T_r - T_w) \tag{14}$$

The total heat flux on the *i* surface is expressed by the formula:

$$Q_i = q_{av,i} S_i \tag{15}$$

where:
$q_{śr,i}$ – average heat flux density on *i* inner surface (of the tip and dome),
S_i – outer surface (tip and dome).

The heat flux density through the inner surface is:

$$q_{w,i} = \frac{Q_i}{S_{w,i}} \tag{16}$$

where:
$S_{w,i}$ – inner surface (of the tip and dome).

For the computations in the ANSYS system, it was assumed that the heat load, i.e., the values of temperature and heat transfer coefficient for every point on the surface change linearly between the initial and final conditions in a given step (1 and 2). 300K (27°C) was assumed as the initial temperature of the structure (at the time of the rocket launch).

3.5. Unsteady heat transfer calculation results

Unsteady heat transfer in the head was calculated using the ANSYS solver. External loads were divided into two steps, according to the flight conditions defined above. Due to the need to assume wall temperature, several iterations were necessary in order to obtain result convergence.

Tab. 4. The laminate's final temperature change in subsequent iterations. Difference calculated in relation to absolute zero [Rosłowicz, 2014]

1 load step			
T_{lam}, K	Assumption	Results	Difference in %
1	300	674	116
2	674	463	28
3	463	546	18
4	546	507	7
5	507	521	3

2 load step			
T_{lam}, K	Assumption	Results	Difference in %
1	520	408	27
2	408	436	6
3	436	429	2

Tab. 5. Heat flux density final values [W/m^2] [Rosłowicz, 2014]

Tip bottom surface	1 000 000	-305
Inner composite surface	284 000	-35 300

The result after second load step means a change of the heat flow direction (from the inside to the outside). It is in line with the expectations, since at that point of the flight, the rocket structure should be cooling down.

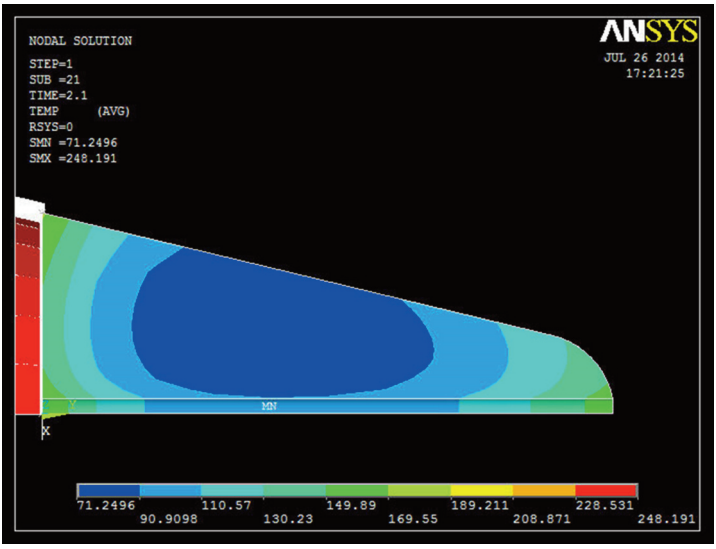

Fig. 21. Temperature field in the tip after 1 load step (simulation time 2.1s; flight time 2.78s). Values stated in °C [Rosłowicz, 2014]

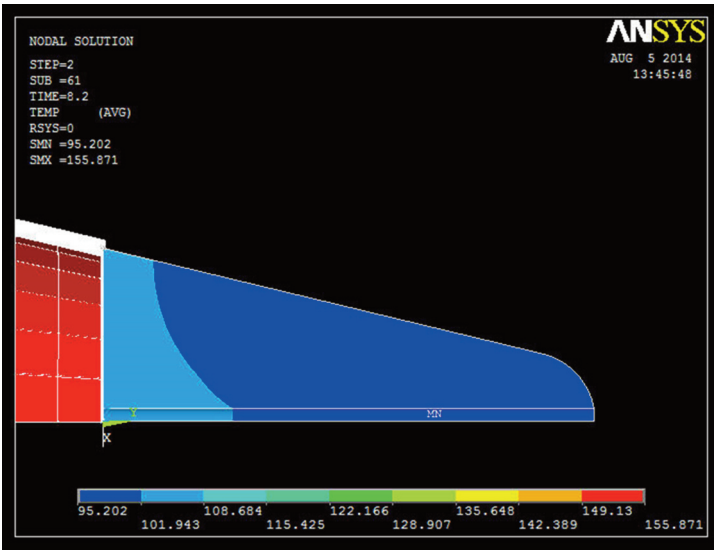

Fig. 22. Temperature field in the tip after 2 load step (simulation time 8.2s; flight time 8.86s) [Rosłowicz, 2014]

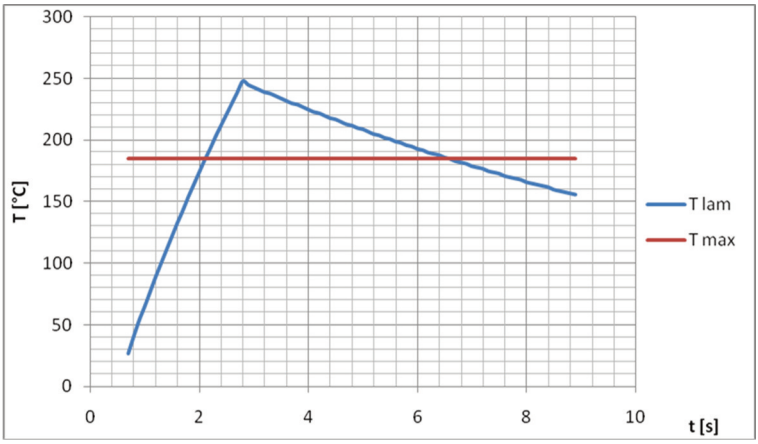

Fig. 23. The laminate surface temperature change T_{lam} (axis y) during the flight of the rocket (axis x). The T_{max} allowable temperature was marked [Rosłowicz, 2014]

4. CONCLUSIONS

The conducted analysis showed significant (up to ca. 250°C for the dome and up to ca. 150°C for the tip) heating of the rocket's structural elements, exposed to direct contact with stagnated air. The brass tip has low thermal resistance (the Biot number around 0.4), so heat is rapidly transported into the structure. It may cause excessive heating of elements located below. The epoxy-resin composite heats up faster (the Biot number in the order of several dozen). Heat is absorbed by resin and slowly transported inside. The analysis of computation results showed the need to use additional thermal protection of the composite part of the head. The flight time, during which excessive heating is present, is about 4.5s. The approximate and simplified nature of the calculations requires also to be taken into account. Due to lack of material data, the heat transfer between the tip and the composite was practically not taken into account (the contact resistance coefficient unknown). In fact, heat transport from brass and from air beyond the culminating point (2 load step) may cause higher laminate temperature, than it can be seen from the above analysis. The further (cylindrical) composite part of the rocket head, which is a transition between the head and the body, is exposed to similar thermal loads.

BIBLIOGRAPHY

[1] Crabtree, L. F., Dommet, R. L., Woodley, J. G., 1970, "Estimation of Heat Transfer to Flat Plates, Cones and Blunt Bodies.", R. & M. No. 3637, Her Majesty's Stationery Office, London

[2] Kaye, J., 1953, "Survey of Friction Coefficients, Recovery Factors and Heat Transfer Coefficients for Supersonic Flow.", Technical Report No. 6418-5, Massachusetts Institute of Technology, Cambridge.

[3] [3] Sekcja Rakietowa SKA, 2014, Wydział Mechaniczny Energetyki i Lotnictwa PW, konsultacja osobista [Rocketry Group of Students' Space Association, 2014, Faculty of Power and Aeronautical Engineering, Warsaw University of Technology, personal consultation]

[4] T. Zagrajek, G. Krzesiński i P. Marek, 2006, *Metoda elementów skończonych w mechanice konstrukcji [The method of finite elements in structural mechanics]*, OWPW, Warszawa.

[5] Firma AMOD, 2014, konsultacja osobista. *[AMOD, 2014, personal consultation]*

[6] Devendra, K., Rangaswamy, T., 2012, "Evaluation of Thermal Properties of E-Glass/ Epoxy Composites Filled by Different Filler Materials",.International Journal of Computational Engineering Research, 2(5), pp. 1708-1714.
[7] Rosłowicz, A., 2013, „Optymalizacja rakiety lecącej na 100km" *[Optimalization of a rocket flying at 100km]*, Praca przejściowa inżynierska, Politechnika Warszawska, Warszawa.
[8] 2012, „Metale kolorowe, mosiądz" *[Non-ferrous metals, brass]*, http://www.dostal.com.pl/metale-kolorowe-mosiadz.html.

ANALIZA WYMIANY CIEPŁA W GŁOWICY RAKIETY NADDŹWIĘKOWEJ

Streszczenie

Niniejszy artykuł zawiera opis metody oraz wyniki numerycznej symulacji wymiany ciepła w elementach głowicy rakiety. Punkt wyjścia stanowiły założone warunki lotu (3 punkty charakterystyczne określone przez wysokość i liczbę Macha) iwyznaczone niezależnie adiabatyczne pole temperatury gazu. Do wyznaczenia pola temperatur na powierzchni rakiety użyty został system ANSYS Fluent. Zostały obliczone przypadki przepływu lepkiego i nielepkiego (dla porównania). Na podstawie wyników dla przypadku lepkiego sformułowano warunki brzegowe wymiany ciepła, założenia modelu numerycznego. Model ograniczono do mosiężnej części noskowej i fragmentu kompozytowej kopułki. Metodą analityczno-empiryczną „średniej entalpii" (intermediate enthalpy) wyznaczono rozkład współczynnika przejmowania ciepła na powierzchni rakiety. Następnie dokonano obliczenia nieustalonej wymiany ciepła z wykorzystaniem systemu ANSYS. Obejmowały one zakres od startu rakiety, poprzez moment osiągnięcia maksymalnej liczby Macha, do wystarczającego schłodzenia konstrukcji. Efektem pracy było sformułowanie wniosków istotnych z punktu widzenia dalszych prac konstrukcyjnych. Wykazano nadmierne ogrzewanie elementów kompozytowych w trakcie lotu.
Słowa kluczowe: technika rakietowa, numeryczna mechanika płynów, nieustalona wymiana ciepła, oprogramowanie ANSYS.